In situ SECM study on concentration profiles of electroactive species from corrosion of stainless steel

M. Zhao, Z. H. Qian, R. J. Qin, J. Y. Yu, Y. J. Wang and L. Niu*

The corrosion behaviours of type 304 stainless steel in acidic chloride solutions were investigated by cyclic voltammetric (CV) measurements at a scanning electrochemical microscope (SECM) tip combined with SECM scan imaging techniques. The results showed that the detection of electroactive species (i.e. ferrous ions) originating from the corrosion process can be accomplished as a function of position of the SECM tip above the stainless steel sample. Moreover, the variation in the tip–sample distance would allow for the tip current to be quantitatively correlated with the concentration profiles of the electroactive species or the related electrochemical activities on the sample surface. In a word, both voltammetric characteristic and three-dimensional SECM imaging related to the corrosion behaviours of 304 stainless steel will be helpful to clarify the possible pathways and reaction mechanisms involved in the corrosion processes.

Keywords: Corrosion, Stainless steel, SECM, Electroactive species, Concentration profiles

Introduction

Corrosion of metals in an aggressive medium would lead to serious damages to structural materials and consequently give rise to tremendous economic losses. Therefore, the macroscopic phenomena and microscopic mechanisms and dynamics of corrosion are of great fundamental interests in the field of corrosion science and engineering.[1]

As tools to approach macroscopic and geometrically averaged information of corrosion processes, traditional electrochemical techniques such as polarisation curves, electrochemical impedance spectroscopy and electrochemical noise are good at providing insight into global corrosion rates and lifetime prediction, but cannot offer much details about the localised dynamics of corrosion processes. To overcome the limitations of the traditional electrochemical techniques, several local electrochemical measurement techniques such as scanning reference electrode technique,[2–4] scanning vibrating electrode technique,[2,5–7] local electrochemical impedance spectroscopy,[2,8,9] scanning Kelvin probe,[2,10,11] electrochemical microcell technique[2,12,13] and scanning electrochemical microscopy (SECM)[2,14–17] have been developed and utilised widely to real time study of localised electrochemical reactions on metal surfaces. Especially, the SECM, as a very powerful technique with high spatial resolution and electrochemical sensitivity (or chemical specificity), usually provided very interesting information concerning the topography and redox activity of the metal/electrolyte interface. Its capability both for analysing larger areas of the sample than other *in situ* methods (e.g. electrochemical scanning tunnelling microscopy) and for direct identification of chemical species (i.e. corrosion products) in localised corrosion processes with high lateral resolution would be greatly advantageous.[18] Souto and co-workers recently reviewed the uses of scanning electrochemical microscopy in corrosion research[16] and reported a variety of studies on the application of the SECM to the examination of organic coatings on metallic substrates,[19–22] the imaging metastable pits on austenitic stainless steel,[23] as well as the imaging redox active species during corrosion processes.[24] Völker *et al.*[25] used SECM to examine '*in situ*' the release of iron ions at the metal/coating interface as direct evidence of metal dissolution and concluded that SECM is a powerful technique for the identification of corrosion products in localised corrosion processes with high lateral resolution. Zhu *et al.*[26] reported the SECM observation of a precursor state to pitting corrosion of stainless steel. In addition, Katemann *et al.*[27] visualised the precursor sites for localised corrosion on lacquered tinplates by means of ac-SECM. Using I^-/I_3^- redox couple as a mediator for sulphide oxidation in the method of amperometric detection, Paik *et al.*[28] and Lister *et al.*[18,29] both showed that dissolution of sulphur inclusions was responsible for the initiation of pitting corrosion of stainless steels by SECM detection. Recently, our group also reported the application of SECM in the study on corrosion processes and mechanisms of metals.[17,30] Up to now, admittedly, the corrosion

Key Laboratory of Colloid and Interface Chemistry, Ministry of Education, School of Chemistry and Chemical Engineering, Shandong University, Jinan 250100, China

*Corresponding author, email lniu@sdu.edu.cn

Published by Maney on behalf of the Institute
Received 7 July 2012; accepted 1 November 2012
DOI 10.1179/1743278212Y.0000000066

mechanisms and dynamics associated with concentration profile of the corrosion products and/or electrochemical activity distribution on the sample surface seem to be not fully understood and clarified, which undoubtedly is an unfavourable factor for the purpose to ultimately elucidate corrosion phenomena and predict corrosion rates.

In the present study, the corrosion performance of 304 stainless steel was investigated by cyclic voltammetric (CV) measurements at SECM tip combined with SECM scan imaging methods. The detection of the electroactive species (i.e. ferrous ions) was accomplished as a function of position of the SECM tip above the steel sample under investigation. In principle, the variation in the tip–sample separation would certainly lead to changes of the current flowing at the tip, thus allowing for the tip current to be quantitatively correlated with the local concentration of the electroactive species at that location and/or the electrochemical activity on the stainless steel surface. The objective of the present study is to fully elucidate the reasonable pathways and reaction mechanisms involved in the corrosion of stainless steel in chloride solution.

Experimental

Chemicals and samples

Chemicals in analytical grade (Aldrich, USA) were used as received. All solutions used were prepared with ultrapure water ($\sim$18 MΩ; Milli-Q system). The sample, type 304 stainless steel (Baosteel, China), was cut from a steel rod (2 mm diameter).

Instruments and procedures

A detailed description of the SECM system was previously reported.[30] The SECM (SECM 270, Uniscan Instruments Ltd, UK) was employed to perform SECM area scan imaging and cyclic voltammetric (CV) measurements. The tip used for the area scan imaging and CV measurements was a glass insulated, disc shaped Pt microelectrode (RG=8), which was fabricated from a Pt wire with 25 μm diameter. The steel sample was mounted into an epoxy resin sleeve, such that only the circular end surface formed the testing face (substrate electrode). Before each experiment, the substrate electrode was ground mechanically with SiC paper to no. 2000 grit finish, and the Pt tip was polished with 0·3 and 0·05 μm γ-alumina powder and then cleaned thoroughly with ultrapure water before use. A saturated calomel electrode was used as a reference electrode and a Pt wire as a counter electrode. All the potentials in the experiments were referred to saturated calomel electrode. The electrochemical cell with the specimen press fitted at its bottom hole was mounted on the three-axis positioning translation stage. The specimen was mounted horizontally facing upwards. A video microscope (charge coupled device) was employed to aid in accurately positioning the tip over the substrate by comparison between the image dimension of the Pt wire and that of the tip–substrate distance. The SECM scan imaging and CV measurements were performed with the tip at different heights over the substrate. The potentials of the tip and the substrate were controlled separately by a bipotentiostat (PG 580, USA). All measurements were performed at ambient temperature in the naturally aerated solutions.

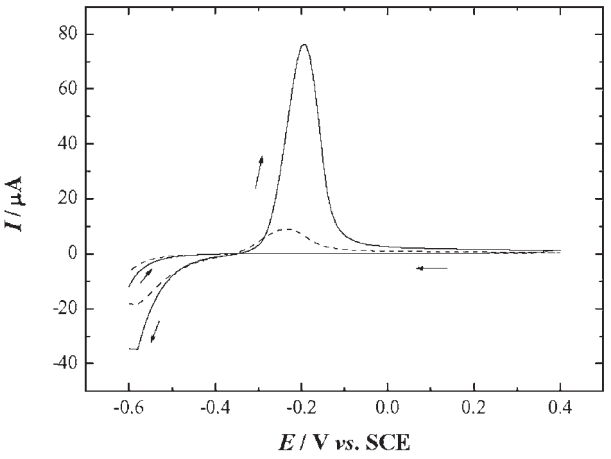

1 Potentiodynamic polarisation curves of 304 stainless steel in 0·5M H_2SO_4+0·1M NaCl solution; scan rate, 10 mV s^{-1}; dot line, sample as received; solid line, sample anodically prepolarised

Results and discussion

Potentiodynamic polarisation curves of stainless steel

Figure 1 shows the potentiodynamic polarisation curves of the stainless steel electrode in 0·5M H_2SO_4+0·1M NaCl solution. The potentiodynamic polarisation measurements were conducted on the same stainless steel electrode with different initial states. The first was the freshly polished steel electrode, while the second steel electrode was initially polarised at +0·9 V (in the transpassive range of the material) for 300 s in 0·1M NaCl solution. Clearly, the polarisation curves of the two electrodes display different voltammetric characteristics, particularly in the behaviours during anodic oxidation process.[31] On the freshly polished steel electrode, the current peak corresponding to anodic oxidation around −0·25 V seems to be small (dot line), while on the electrode with an initial potentiostatic polarisation, the current peak of anodic oxidation rises greatly and shifts to a more positive potential around −0·2 V (solid line). The initial potentiostatic polarisation for the second steel electrode before measuring the potentiodynamic polarisation curves would probably lead to expectable surface roughening with increased area to take part in the subsequent anodic oxidation process during the potentiodynamic polarisation, definitely resulting in more considerable corrosion on the steel surface with greater current peak (solid line), compared with the outcome on the freshly polished steel electrode, namely a slight corrosion with lower current peak (dot line).

Cyclic voltammograms measured at Pt tip

As reported previously, the SECM tip is sensitive to the presence of a dissolved electroactive species, either a reactant or a corrosion product, in solution.[24] In this section, a CV measurement at the SECM tip was performed as a function of the presence of Fe^{2+} to confirm that the increase in SECM tip currents was due to the contribution of electroactive species (i.e. Fe^{2+} ions).[19] As can be seen in Fig. 2, each current plateau within the potentials from +0·5 to +0·7 V varied with corresponding concentration of Fe^{2+} ions in the solution and exhibited regular trends as can

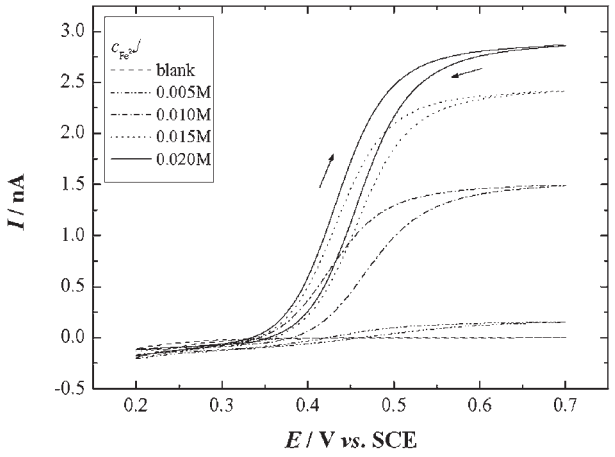

2 Cyclic voltammogram measured at SECM Pt tip in 0·5M H_2SO_4+0·1M NaCl solution containing different concentrations of Fe^{2+} ions; scan rate, 10 mV s^{-1}

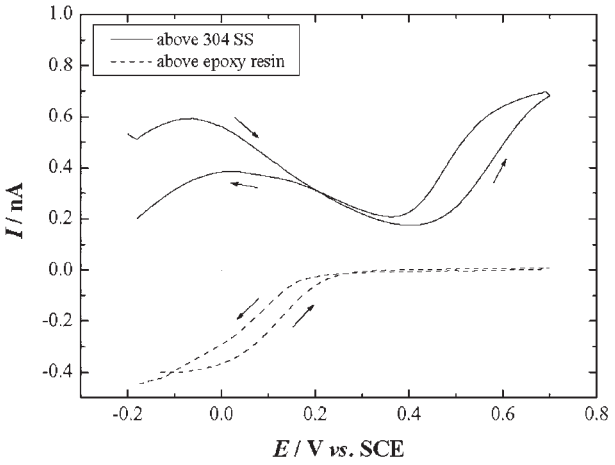

3 Cyclic voltammogram measured at SECM Pt tip in 0·5M H_2SO_4+0·1M NaCl solution above stainless steel or epoxy substrate; scan rate, 10 mV s^{-1}; tip–substrate distance, 5 μm

be expected, i.e. the higher the concentration of Fe^{2+} ions, the larger the diffusion limited current on the tip. In other words, the CVs on the one hand show the dependence of diffusion limited current on the concentrations of electroactive species (i.e. Fe^{2+} ions) in the solution, which follows the equation (1) of the steady state current at a disc microelectrode[14]

$$I_{tip} = 4nFDcr \quad (1)$$

where r is the microelectrode radius, F is the Faraday constant, D is the diffusion coefficient and c is the concentration of electroactive species. On the other hand, it allows a reasonable potential value of +0·60 V to be deduced for the diffusion limited oxidation of Fe^{2+} ions in this solution.[25] This potential will be applied in polarisation on Pt tip in the following experiment of SECM imaging.

On the basis of the correlation of tip current with electroactive species (i.e. Fe^{2+} ions) presented in the solution (see Fig. 2), subsequent CV measurements at the SECM tip close to the substrate (i.e. steel or epoxy resin) at open circuit corrosion potential were performed in acidic chloride solutions in order to investigate the effect of nature of the substrate (i.e. a conductor or an insulator) on the voltammetric characteristics of the tip, as shown in Fig. 3. It is worth noting that marked differences existed between the voltammetric behaviours of the tip above steel substrate (solid line) and that above the epoxy resin (dot line). When the tip was located above the conductive steel surface at a height of 5 μm, the tip currents varied significantly with sweeping potentials during the CV measurements, probably corresponding to different electrochemical reactions described as follows. On the one hand, the current peak around −0·1 V may be related to the oxidation of hydrogen peroxide formed during the reduction in oxygen at the cathodic sites in the aerated aqueous solution,[23,32] while the current peak appearing at potential more positively than 0·4 V may come from the diffusion limited current of electroactive species (i.e. Fe^{2+} ions) produced by the anodic dissolution of steel in the chloride solution.[24] On the other hand, when the tip was located above the epoxy sleeve (i.e. an insulator) with the same height of 5 μm, however, much different voltammetric behaviours were exhibited on the tip (dot line, Fig. 3). That is, a smaller current peak around −0·1 V related to oxygen electroreduction still existed, while the current peak at potentials more positively than 0·4 V became ultimately unremarkable.

As we know, the dissolved oxygen existed uniformly in the solution, no matter how far from the steel or epoxy resin substrate. For the electroactive species, Fe^{2+} ions, however, the situation would be to some extent different. There was certainly a concentration gradient of Fe^{2+} ions, originated from the anodic dissolution of steel, in the regions from steel substrate to insulating epoxy resin sleeve. Namely, the farther from the surface of steel, the lower the concentration of the species of Fe^{2+} ions. Therefore, for the CV measurements at the SECM tip close to the epoxy resin sleeve substrate, as can be expected, the epoxy resin (i.e. insulating sleeve) actually acted as an obstacle towards both oxygen electroreduction and the diffusion limited oxidation of Fe^{2+} ions at the tip, corresponding to the subsequent reduction in the anodic and cathodic current peaks (dot line, Fig. 3), compared to more remarkable current peaks that appeared in the CV measurements at the SECM tip close to the steel substrate as shown in Fig. 3 (solid line).

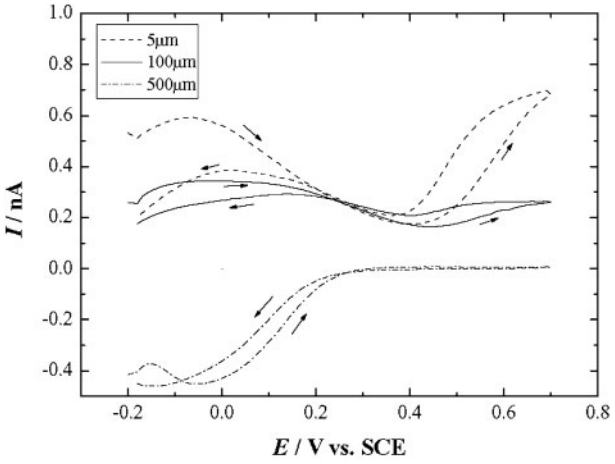

4 Cyclic voltammogram measured at SECM Pt tip in 0·5M H_2SO_4+0·1M NaCl solution above stainless steel substrate; scan rate, 10 mV s^{-1}; tip–substrate distance, 5, 100 and 500 μm

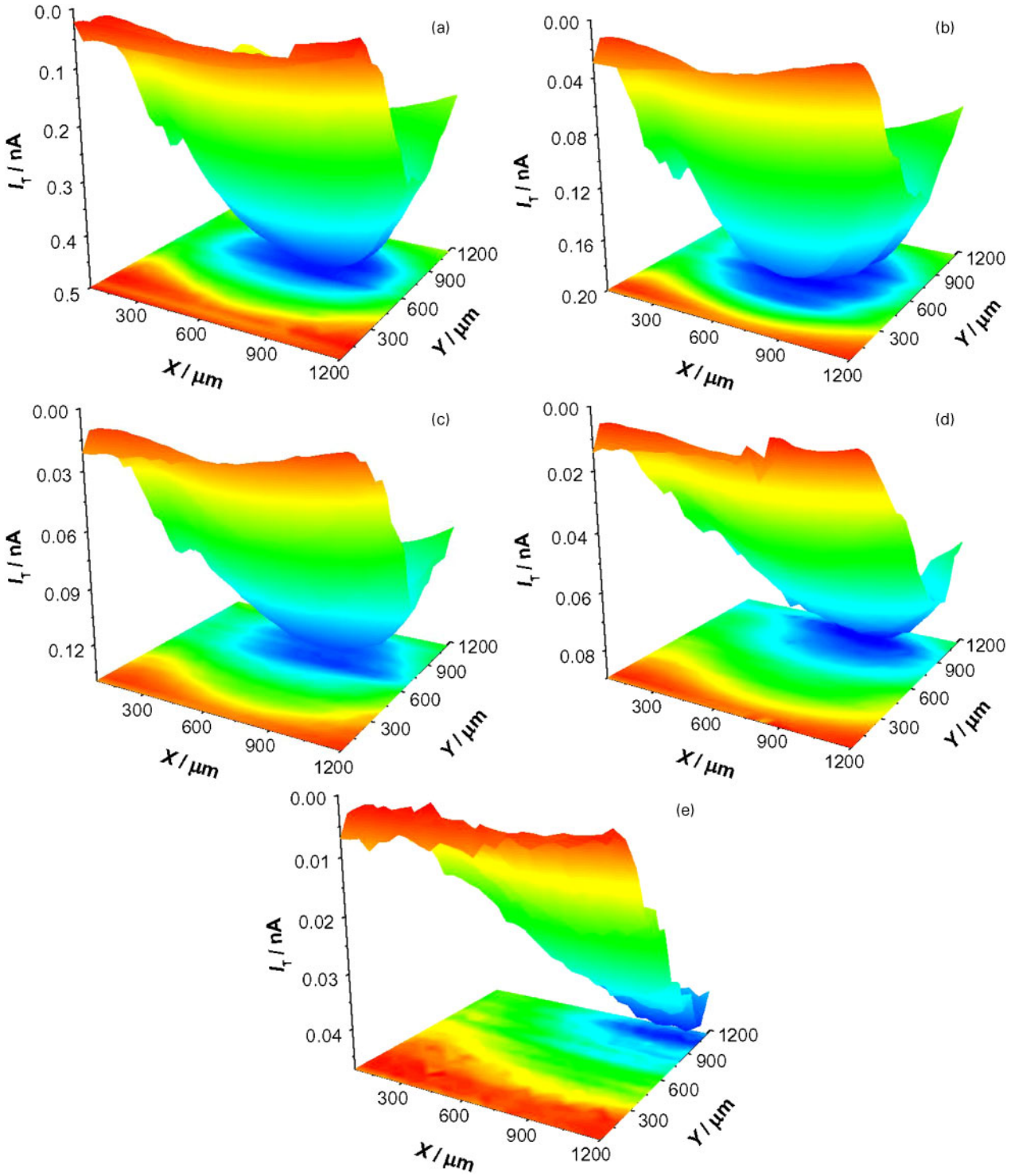

5 Images (SECM) of 304 stainless steel at open circuit corrosion potential in 0·5M H_2SO_4+0·1M NaCl solution. Tip–substrate distance: *a* 5 μm, *b* 15 μm, *c* 50 μm, *d* 100 μm and *e* 200 μm. E_{tip}=+0·6 V. Scan rate of tip over specimen surface was generally 60 μm s^{-1} in *x* direction

In order to study the ability for the SECM tip to detect the local concentration of dissolved species (i.e. Fe^{2+} ions) produced during actual corrosive process of steel in the NaCl solution, the SECM tip, employed as a working electrode, was placed directly above the steel surface at different heights achieved by means of the assistance of the video microscope (charge coupled device), and CV measurement was subsequently conducted, as shown in Fig. 4. Of the three curves, the dash line traces a voltammogram acquired while the tip microelectrode was placed 5 μm above the surface, and the solid and dash dot lines trace voltammograms collected at the tip when it was positioned 100 and 500 μm above the steel surface (i.e. the active sites) respectively. Evidently, it is interesting to note that the tip current, which is directly related to the actual concentration of Fe^{2+} ions in the solution, was highly dependent on the distance from the tip to steel sample. As already known, it is to be expected that with increasing distance between tip and substrate, the amount

of the electroactive species that diffused to the tip diminished and consequently led to the fall of the steady state diffusion currents.[24] Conversely, if the distance between tip and substrate becomes shorter, the decreasing diffusion path from substrate to tip in this case would promote the diffusion of corrosion product (i.e. Fe^{2+} ion) to the tip more easily and effectively, in comparison with that in the case of a longer tip–substrate distance. This conclusion will be testified in the following SECM scan imaging experiments.

Scanning electrochemical microscopy scan imaging of stainless steel

Figure 5 shows the steady state currents monitored at the SECM tip during area scan imaging measurements when the tip was polarised at $+0{\cdot}60$ V and crossed at various heights over the steel specimen at open circuit corrosion potential ($E_{OCP}=-0{\cdot}645$ V). As can be seen in Fig. 5, all the tip currents were anodic in nature and varied significantly with the tip–substrate distance. When the tip–substrate distances increased gradually from 5, 15, 50, 100 to 200 μm, the tip currents decreased distinctly while the three-dimensional SECM imaging maintained almost the same pattern, except the situation with farther distances between tip and substrate. Another feature regarding the SECM imaging in Fig. 5 is that, accompanying with the increases of the tip–substrate distance, the coordinates for the maximum activity seem to shift to the top right in the image.

As earlier indicated, the current detected at a micrometric probe will be indicative of concentrations averaged over micrometric distances, i.e. true local concentration of a species will be monitored.[33] In addition, as discussed before, the ionic species resulting from the anodic oxidation of a metal may be detected at the SECM tip by adequately selecting a potential value at which they are either reduced or further electro-oxidised.[21] In Fig. 5, the area scan imaging results through SECM operation in sample generation-tip collection (SG-TC) mode demonstrated that within certain distances between the tip and the steel substrate, the concentration of Fe^{2+} ions emanating from the dissolving electrode could be determined at the SECM tip. That is, the area scan images show the concentration profile of Fe^{2+} ions as a function of tip–substrate distances. These observations are consistent with the conclusions reported earlier as mentioned above. On the other hand, since the grid dimensions ($1{\cdot}2 \times 1{\cdot}2$ mm) was included in the circular section of the stainless steel wire, it could be expected that the higher concentrations of Fe^{2+} species would be detected at the centre of the sample, due to the fact that the steel specimen corroded somewhat homogeneously. However, the unusual shifts in coordinates for the maximum activity, to the top right in the SECM image, with increasing distances between tip and substrate may be attributed to the following causes. Since each area scan image was obtained by a series of combined linescans above the specimen, the scanning tip with certain scan rate would to some extent agitate the solution containing Fe^{2+} species, resulting in the shifts in the concentration profiles of the electroactive species or, in other word, the corresponding coordinates for the maximum activity in Fig. 5. Generally, the longer the distance between tip and substrate, the fewer the amount of Fe^{2+} species to reach the tip surface and to be electro-oxidised further, which lead to the reduction in the tip current and more obvious shift in the maximum activity to the top right direction in the SECM image. In a word, the above observations seem to be in agreement with the conclusive remarks that mapping of concentration profiles of redox active species participating in corrosion processes at the open circuit corrosion potential can be performed with great accuracy and resolution using the SECM.[23,24]

Conclusions

1. By means of the advantages of substrate generation-tip collection (SG-TC) mode in SECM operation, both CVs measured at the tip and the SECM scan imaging above the steel substrate can be useful to online monitor the products (i.e. electroactive species) resulting from corrosion processes.

2. The detection of the electroactive species (i.e. Fe^{2+} ions) originating from the corrosion process of 304 stainless steel in acidic chloride solutions can be achieved by setting the tip at an appropriate position above the steel substrate under investigation, allowing for in principle the tip current to be quantitatively correlated with the concentration profiles of the electroactive species or the electrochemical activities on the steel surface.

Acknowledgements

This work was supported by the National Natural Science Foundation of China (grant no. 51171094), the Natural Science Foundation of Shandong Province of China (grant no. 2009ZRB01965) and the National Basic Research Program of China (grant no. 2009CB930103).

References

1. H. H. Strehblow and P. Marcus: in 'Corrosion mechanisms in theory and practice', (ed. P. Marcus), 1–104; 2012, Boca Raton, FL, CRC Press.
2. R. Oltra: in 'Local probe techniques for corrosion research', (ed. R. Oltra *et al.*), 1–11; 2007, Cambridge, Woodhead Publishing Limited.
3. M. Khobaib, A. Rensi, T. Matakis and M. S. Donley: *Prog. Org. Coat.*, 2001, **41**, 266–272.
4. B. T. Lu, Z. K. Chen, J. L. Luo, B. M. Patchett and Z. H. Xu: *Electrochim. Acta*, 2005, **50**, 1391–1403.
5. H. Krawiec, V. Vignal and R. Oltra: *Electrochem. Commun.*, 2004, **6**, 655–660.
6. A. M. Simões, A. C. Bastos, M. G. Ferreira, Y. González-García, S. González and R. M. Souto: *Corros. Sci.*, 2007, **49**, 726–739.
7. A. C. Bastos, M. L. Zheludkevich and M. G. S. Ferreira: *Prog. Org. Coat.*, 2008, **63**, 282–290.
8. B. B. Katemann, A. Schulte, E. J. Calvo, M. Koudelka-Hep and W. Schuhmann: *Electrochem. Commun.*, 2002, **4**, 134–138.
9. M. C. Li and Y. F. Cheng: *Electrochim. Acta*, 2008, **53**, 2831–2836.
10. A. P. Nazarov and D. Thierry: *Electrochim. Acta*, 2004, **49**, 2955–2964.
11. J. M. Sykes and M. Doherty: *Corros. Sci.*, 2008, **50**, 2773–2778.
12. T. Suter and H. Böhni: *Electrochim. Acta*, 1998, **43**, 2843–2849.
13. C. Garcia, M. P. de Tiedra, Y. Blanco, O. Martin and F. Martin: *Corros. Sci.*, 2008, **50**, 2390–2397.
14. A. J. Bard: in 'Scanning electrochemical microscopy', (ed. A. J. Bard and M. V. Mirkin), 1–16; 2001, New York, Marcel Dekker Inc.
15. G. Wittstock, M. Burchardt, S. E. Pust, Y. Shen and C. Zhao: *Angew. Chem. Int. Ed.*, 2007, **46**, 1584–1617.
16. R. M. Souto, S. V. Lamaka and S. González: in 'Microscopy: science, technology, applications and education', (ed. A. Méndez-Vilas and J. Díaz), 1769–1780; 2010, Badajoz, Formatex.
17. L. Niu, Y. H. Yin, W. K. Guo, M. Lu, R. J. Qin and S. H. Chen: *J. Mater. Sci.*, 2009, **44**, 4511–4521.

18. T. E. Lister and P. J. Pinhero: *Electrochem. Solid-State Lett.*, 2002, **5**, B33–B36.
19. A. C. Bastos, A. M. Simões, S. González, Y. González-García and R. M. Souto: *Prog. Org. Coat.*, 2005, **53**, 177–182.
20. R. M. Souto, Y. González-García, S. González and G. T. Burstein: *Corros. Sci.*, 2004, **46**, 2621–2628.
21. R. M. Souto, Y. González-García and S. González: *Corros. Sci.*, 2005, **47**, 3312–3323.
22. R. M. Souto, Y. González-García, J. Izquierdo and S. González: *Corros. Sci.*, 2010, **52**, 748–753.
23. Y. González-García, G. T. Burstein, S. González and R.M. Souto: *Electrochem. Commun.*, 2004, **6**, 637–642.
24. A. C. Bastos, A. M. Simões, S. González, Y. González-García and R. M.Souto: *Electrochem. Commun.*, 2004, **6**, 1212–1215.
25. E. Völker, C. G. Inchauspe and E. J. Calvo: *Electrochem. Commun.*, 2006, **8**, 179–183.
26. Y. Zhu and D. E. Williams: *J. Electrochem. Soc.*, 1997, **144**, L43–L45.
27. B. B. Katemann, C. G. Inchauspe, P. A. Castro, A. Schulte, E. J. Calvo and W. Schuhmann: *Electrochim. Acta*, 2003, **48**, 1115–1121.
28. C. H. Paik, H. S. White and R. C. Alkire: *J. Electrochem. Soc.*, 2000, **147**, 4120–4124.
29. T. E. Lister and P. J. Pinhero: *Electrochim. Acta*, 2003, **48**, 2371–2378.
30. Y. H. Yin, L. Niu, M. Lu, W. K. Guo and S. H. Chen: *Appl. Surf. Sci.*, 2009, **255**, 9193–9199.
31. M. Keddam: in 'Corrosion mechanisms in theory and practice', (ed. P. Marcus), 149–215; 2012, Boca Raton, FL, CRC Press.
32. S. González, J. J. Santana, Y. González-García, L. Fernández-Mérida and R. M. Souto: *Corros. Sci.*, 2011, **53**, 1910–1915.
33. N. Baltes, L. Thouin, C. Amatore and J. Heinze: *Angew. Chem. Int. Ed.*, 2004, **43**, 1431–1438.